Role of MR imaging in chronic wrist pain

Zanetti, Marco ; Saupe, Nadja ; Nagy, Ladislav

DOI: https://doi.org/10.1007/s00330-006-0365-4

Eur Radiol (2007) 17: 927–938
DOI 10.1007/s00330-006-0365-4

Marco Zanetti
Nadja Saupe
Ladislav Nagy

Role of MR imaging in chronic wrist pain

Received: 6 April 2006
Revised: 19 May 2006
Accepted: 12 June 2006
Published online: 24 August 2006

M. Zanetti (✉) · N. Saupe
Department of Radiology,
University Hospital Balgrist,
Forchstrasse 340,
8008 Zurich, Switzerland
e-mail: marco.zanetti@balgrist.ch
Tel.: +41-44-3863303
Fax: +41-44-3863319

L. Nagy
Department of Orthopedic Surgery,
University Hospital Balgrist,
Forchstrasse 340,
8008 Zurich, Switzerland

Abstract Magnetic resonance (MR) imaging for chronic wrist pain is challenging. Correct assessment of the triangular fibrocartilage, hyaline cartilage, ligaments, and tendons has become mandatory for comprehensive decision making in wrist surgery. The MR technique, potential and limits of MR imaging in patients with chronic wrist pain will be discussed. MR arthrography with injection of gadolinium-containing contrast material into the distal radioulnar joint is suggested for evaluation of the triangular fibrocartilage. The clinically meaningful ulnar-sided peripheral tears are otherwise hard to diagnose. The diagnostic performance of MR imaging for interosseous ligament tears varies considerably. The sensitivity for scapholunate ligament tears is consistently better than for lunotriquetral ligament tears. Gadolinium-enhanced MR imaging is considered to be the best technique for detecting established avascularity of bone, but the assessment of the MR results remains challenging. Most cases of ulnar impaction syndrome have characteristic focal signal intensity changes in the ulnar aspect of the lunate. Avascular necrosis of the lunate (Kienböck's disease) is characterized by signal changes starting in the proximal radial aspect of the lunate. MR imaging is extremely sensitive for occult fractures. Questions arise if occult posttraumatic bone lesions seen on MR images only necessarily require the same treatment as fractures evident on plain films or computed tomography (CT) images. MR imaging and ultrasound are equally effective for detecting occult carpal ganglia. Carpe bossu (carpal boss) is a bony protuberance of a carpometacarpal joint II and III which may be associated with pain.

Keywords Triangular fibrocartilage · Wrist, ligaments · Ganglia · Occult fractures · Ulnar impaction · Kienböck's disease · Carpal boss

Introduction

Standard radiographs and three-compartment arthrography has historically been the standard for imaging when evaluating chronic wrist pain [1, 2]. More recently, magnetic resonance (MR) imaging has taken a leading role in wrist imaging. The MR technique, potential and limits of MR imaging in patients with chronic wrist pain will be discussed.

Technical considerations

Optimal MR imaging of the wrist is best performed on a high-field-strength magnet with a dedicated wrist coil. As the wrist joint is relatively small, a dedicated wrist surface coil, thin (2–3 mm) sections and a small (8–10 cm) field of view are required to consistently diagnose pathologic conditions of the structures in the wrist. As comfortable patient positioning is necessary to reduce motion, some

radiologists prefer imaging the wrist with the arm at the patient's side. As more homogenous signals are generated in the center of the magnet, most institutions [3–6] examine the patient with the arm above his head and with the hand pronated ("Superman position"). Attention should be paid to avoid excessive radial or ulnar deviation, as this will affect normal sagittal radiolunocapitate alignment, tempting to erroneously diagnose carpal instability patterns. Moreover, these parameters have been defined and validated for conventional radiographs only [7] and not for sections of the wrist as obtained by tomography, computed tomography(CT) or MR imaging. A dorsal intercalated segmental instability (DISI) can be mimicked on sagittal MR images even in correctly positioned wrists. The lunate appears more dorsally tilted on sagittal MR images than on lateral radiographs [8].

In our institution, direct MR arthrography is performed by starting with contrast material injection (0.5 ml iodinated (300 mg/ml) and 0.5 ml 4 mmol/l gadolinium-containing MR contrast material) into the distal radioulnar joint (DRUJ), followed by a second injection into the midcarpal compartment. In patients where the referring clinician asks specifically about cartilage lesions in the radiocarpal joint, an additional radiocarpal joint injection is performed when this joint is not already filled by contrast material from the first two injections. Serial fluoroscopic spot radiographs are taken to document placement and spreading of the contrast material for MR arthrography and to use as conventional wrist arthrograms.

Indirect MR arthrography is based on the concept that contrast material injected intravenously, over time will diffuse into the joint space, so that quasiarthrographic T1-weighted images can be obtained.

There are two physical processes that cause contrast material to move into the joint space: bulk flow and diffusion. Bulk flow is related to the pressure gradient between the vascular system and the joint space. Diffusion is based on the difference in concentration between plasma and joint fluid. Double- and triple-dose intravenous injections have a positive effect on indirect arthrography, but not nearly as much as one might think [9, 10].

For indirect MR arthrography, a dose of 0.1 mmol per kilogram of body weight of gadolinium-containing contrast material is administered intravenously. The injection is performed prior to imaging, and no precontrast images are obtained. Exercise tends to improve the indirect effect. Imaging should be delayed for 5–10 min. If there is hyperemia or synovitis of the structure of interest, these times can be decreased by one-half. However, if there is clinically suspected joint effusion the time should be at least doubled [11].

Recently, 3.0-T MR systems have become available for clinical use. Several studies have demonstrated improved imaging quality and speed in imaging musculoskeletal disorders at 3.0 T as well as an improvement in diagnostic accuracy [4, 12–14]. The performance of the 3.0-T MR systems critically depends on a successful adaptation to the increased absolute chemical shift difference between water and fat, the changed T1 and T2 tissue relaxation times and to a potentially increased radiofrequency specific absorption rate [13]. Recommended changes at 3.0 T to improve image quality include shortening of echo time, increase of repetition time and higher spatial resolution [15].

Triangular fibrocartilage (TFC)

The TFC complex consists of the TFC (also called articular disk), the dorsal and palmar radioulnar ligaments, the ulnocarpal meniscal homologue, the dorsal and palmar ulnocarpal ligaments, the sheath of the extensor carpi ulnaris tendon, and the capsule of the distal radioulnar joint. The ulnar attachment of the TFC is composed of two distinct laminae: the distal lamina is orientated horizontally

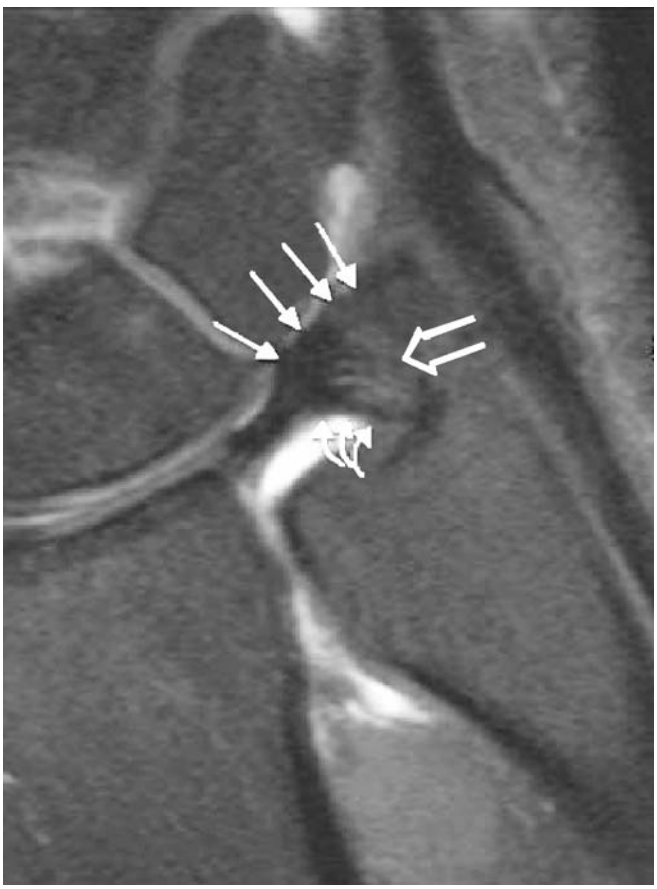

Fig. 1 Normal triangular fibrocartilage. Coronal proton-density-weighted fat-suppressed MR arthrogram demonstrates the normal ulnar attachment of the triangular fibrocartilage, which is composed of two distinct laminae: the distal lamina (*straight arrows*) lies between the articular disc and the styloid process of the ulna and the proximal lamina (*curved arrows*) curves from the undersurface of the articular disc to the ulnar fovea. The fibrovascular tissue (*open arrow*) between the two laminae may mimic an abnormal condition

and extends between the articular disc and the styloid process of the ulna and finally the base of the fifth metacarpal. The proximal lamina is orientated vertically and curves from the undersurface of the articular disc to the ulnar fovea. The two laminae are separated by the ligamentum subcruentum, which represents fibrovascular tissue (Fig. 1).

The TFC acts as a cushion between the distal ulna and the proximal carpal row. The TFC has gained close attention in the radiological and orthopedic literature. Traumatic and degenerative lesions of the TFC are well-accepted causes of wrist pain and efficient treatment options are available. Several studies, including those from the early beginning of musculoskeletal MR imaging [3, 16], have shown excellent correlation between internal derangements at MR imaging and surgery with accuracies up to 100% (Table 1). However, the results vary considerably. Less optimistic results are consistently reported by orthopedic hand surgeons [17–19], while better results are shown by radiologists [5, 20]. Complete tears (Fig. 2) are better visualized than partial tears. Hereby, the location of the TFC lesions is crucial: excellent results are reported for the central or radial TFC lesions [21], but poor results appear in the literature for peripheral TFC lesions at the ulnar insertion [22, 23] (Fig. 3).

The location and configuration of the tear play an important role for the hand surgeons. The Palmer classification [24] is commonly used among orthopedic hand surgeons. The Palmer classification is based on the etiology (traumatic versus degenerative), the location, and extent of the lesion. Palmer divided these into two completely different categories: traumatic (class I) and degenerative (class II). Further subdivisions serve to clarify the location of injury in traumatic lesions and the extent of the cumulative derangement in degenerative lesions.

Table 1 Diagnostic accuracy of MR for complete TFC tears (adapted from [65]; *n.a.* not available)

Reference	Year	*n*	Sensitivity	Specificity	Accuracy
Golimbu et al. [3]	1989	20	1.00	0.86	0.95
Zlatkin et al. [16]	1989	21	0.89	0.92	0.90
Pederzini et al. [66]	1992	11	0.90	1.00	0.91
Schweitzer et al. [67]	1992	15	0.67	1.00	0.80
Lester et al. [18]	1995	14	0.79	n.a.	0.79
Totterman et al. [29]	1996	31	0.92	0.84	0.87
Potter et al. [68]	1997	77	0.88	0.97	0.92
Oneson et al. [26]	1997	56	0.86	0.75	0.80
Johnstone et al.[17]	1997	43	0.80	0.70	0.74
Shionoya et al. [19]	1998	102	0.73	0.72	0.73
Scheck et al. [5][a]	1999	20	0.80	0.60	0.70
Braun et al. [22][a]	2003	75	0.96	1.00	0.99
Schmitt et al. [21][a]	2005	125	0.97	0.96	0.97
Total		610	0.86	0.86	0.85

[a]Direct MR arthrography

Fig. 2 Radial sided central communicating triangular fibrocartilage tear, Palmer class 1A. Coronal T1-weighted fat-suppressed MR arthrogram reveals a radial-sided central communicating triangular fibrocartilage tear (*arrow*)

Palmer stressed that traumatic lesions (class 1 lesions) are slit-like. He separated them from degenerative lesions (class 2) which were more extensive due to TFC wear. Moreover, he classified the traumatic lesions as class 1A when the slit was located 2–3 mm medial to the radial attachment of the TFC, class 1B as avulsion from its

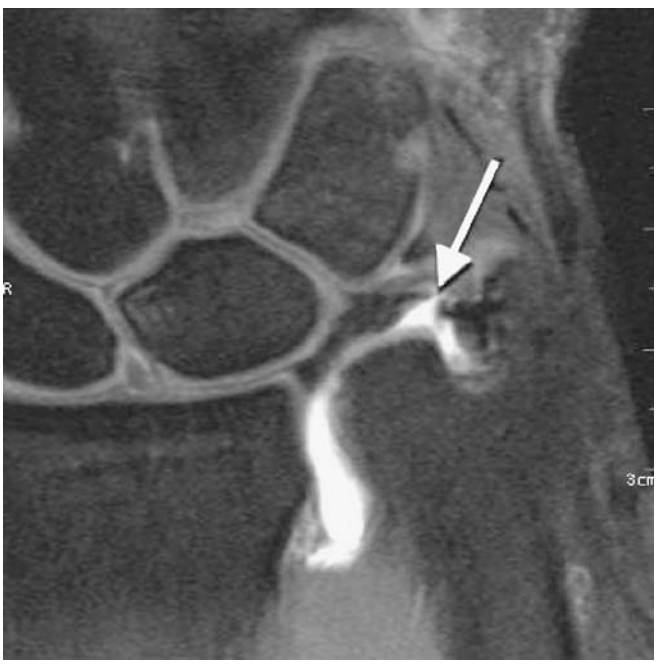

Fig. 3 Ulnar-sided peripheral triangular fibrocartilage tear. Coronal T1-weighted fat-suppressed MR arthrogram demonstrates an ulnar-sided peripheral triangular fibrocartilage tear

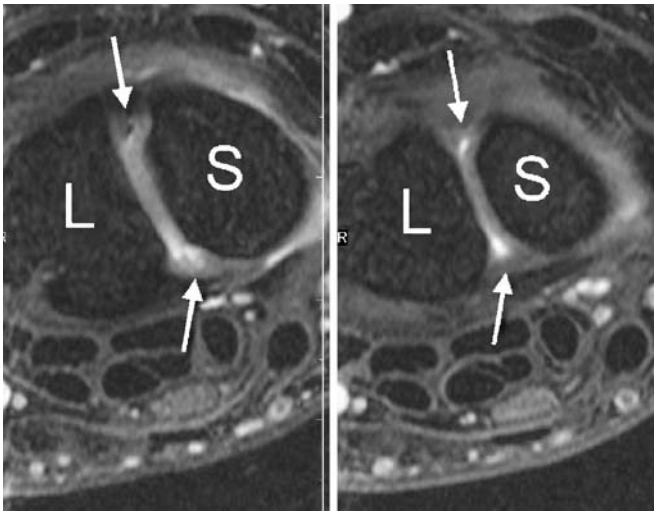

Fig. 4 Normal scapholunate and lunatotriquetral ligament.Two consecutive section of an axial gradient-echo image (True Fisp) demonstrate the normal dorsal and palmar portions (*arrows*) of the scapholunate ligament (*L* lunate, *S* scaphoid)

insertion into the distal ulna, class 1C as avulsion of the TFC from its distal attachment to the lunate or triquetrum, and class 1D as avulsion of the TFC from its attachment at the radius. However, slit-like communicating TFC lesions are also commonly found in contralateral asymptomatic wrists (69%, in Zanetti et al. [25]), questioning the traumatic origin and challenging Palmer's theory. The ulnar-sided peripheral TFC tears have a more consistent correlation with pain than central or radial TFC tears. Moreover, they are most commonly non-communicating and only visible when contrast material is injected into the DRUJ. While excellent results have been reported for depicting central or radial-sided tears (up to 99% accuracy [21, 22]) only poor accuracy was reported for peripheral ulnar attachment tears [23, 26]. Both conventional arthrography (0% sensitivity [27]) and MR imaging (17% sensitivity [23]) may miss TFC ulnar attachment tears. The lower accuracy of MR imaging for peripheral ulnar attachment tears is explained by the presence of vascularized fibrous tissue [28] at this location, resulting in high signal mimicking a tear [23, 29]. MR arthrography with injection of gadolinium-containing contrast material into the DRUJ for evaluation of the TFC should be considered as an appropriate MR technique because accuracy could be raised up to 80% [30] for these clinically meaningful peripheral ulnar-sided tears.

Ligaments

The scapholunate and lunotriquetral ligaments are important stabilizers of the wrist. Anatomically, both ligaments are composed of three distinct components: the volar and dorsal portions consist of transversely oriented collagen fibers that connect the scaphoid and lunate bones and the lunate and triquetral bones, respectively. Between the volar and dorsal portions lies the central segment, which is also known as the proximal or membranous part [31]. Dorsal and palmar segments of both ligaments are stout and strong true ligaments, in contrast to the central membranous segments of both ligaments, whose mechanical properties are almost insignificant [32].

Knowledge of the particular anatomy of these ligaments is important, since the site and extent of a disrupted ligament segment may be used to differentiate between a traumatic tear and a degenerative change [33]. A complete ligamentous disruption or involvement of the dorsal or volar portion of the ligament indicates rather a traumatic origin, whereas central perforations are more compatible with a physiological degeneration [34]. To assess the volar and dorsal portions of the interosseous ligaments, MR images should be analyzed in all three imaging planes. The transverse imaging plane is probably the best (Fig. 4).

Several reports have been published on the diagnostic performance of MR imaging with regard to the detection

Table 2 Accuracies of MR imaging for ligament lesions (adapted from [65]; *n.a.* not available)

			Scapholunate ligament			Lunatotriquetral ligament		
Reference	Year	*n*	Sensitivity	Specificity	Accuracy	Sensitivity	Specificity	Accuracy
Zlatkin et al. [16]	1989	20	0.71	1.00	0.90	0.50	1.00	0.80
Schweitzer et al. [67]	1992	15	0.40	0.60	0.53	0.75	0.64	0.67
Totterrman et al. [69]	1993	8	n.a.	1.00	1.00	1.00	1.00	1.00
Potter et al. [68]	1997	53	0.88	1.00	0.96	0.40	0.97	0.89
Johnstone et al. [17]	1997	43	0.38	1.00	0.88	0.00	0.97	0.84
Scheck et al. [20][a]	1999	20	0.86	0.46	0.60	0.40	0.97	0.89
Braun et al. [22][a]	2003	75	0.83	0.96	n.a.	0.44	0.99	n.a.
Schmitt et al. [21][a]	2005	125	0.92	1.00	0.99	n.a.	n.a.	n.a.
Total		359	0.71	0.88	0.84	0.50	0.93	0.85

[a]Direct MR arthrography

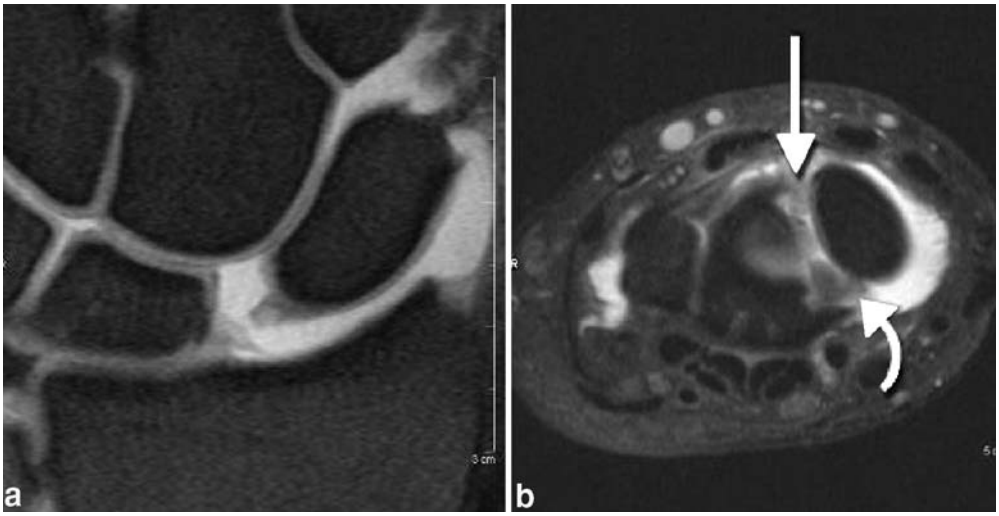

Fig. 5 Scapholunate ligament tear. **a** Coronal proton-density-weighted fat-suppressed MR arthrogram demonstrates widening of the scapholunate space and the tear of the SL ligament in the membranous portion. **b** The axial proton-density-weighted fat-suppressed MR arthrogram demonstrates the scapholunate tear extending into the dorsal (*straight arrow*) and palmar (*curved arrow*) portion of the ligament

of interosseous ligament tears, irrespective of the segmental anatomy. Thus, the true clinical value may not be proportional. The results are summarized in Table 2. Generally, the sensitivity for scapholunate ligament tears (Fig. 5) was consistently better than for lunotriquetral ligament tears.

Tendons

Tendon pathology is often encountered in the wrist and hand, which may be the result of overuse, trauma or inflammation. Normal tendons appear as low signal structures on both T1- and T2-weighted images. With tendinosis, thickening of the tendon and increased signal on T1 weighted images is seen. With partial tears increased signal is visible additionally on T2-weighted images. On imaging and in pathological analyses, there is considerable overlap between both conditions, tendinosis and partial tear. A complete tendon tear is characterized by a complete loss of tendon with retraction. Tenosynovitis is visible as fluid within the tendon sheath, with possible thickening of the sheath itself. On imaging grounds alone, it may be difficult to distinguish inflammatory from infective tenosynovitis. Tenosynovitis of the extensor carpi ulnaris tendon is an important differential diagnosis for ulnar-sided wrist pain. Extensor carpi ulnaris tendon dislocation may be associated with instability of the distal radioulnar joint and is frequently seen in rheumatoid disease [35].

Thickened tendons of the first compartment of the wrist and synovial edema should raise the suspicion of de Quervain's synovitis (Fig. 6). De Quervain's stenosing tenosynovitis affects the first most radial of the six separate synovial lined extensor tendon compartments formed by

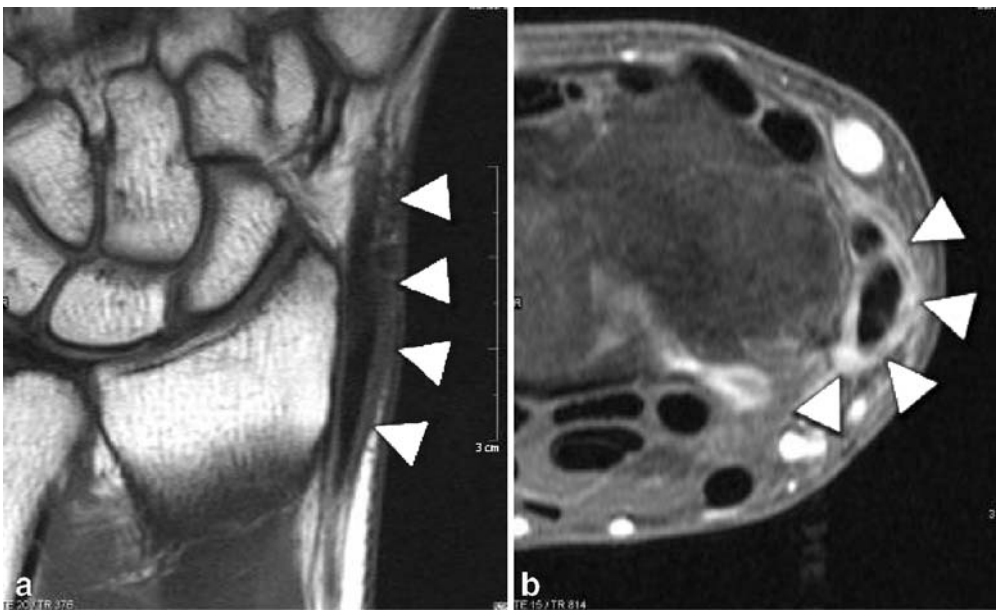

Fig. 6 De Quervain's synovitis. The coronal T1-weighted (**a**) and the axial gadolinium enhanced fat suppressed T1-weighted (**b**) MR images demonstrate the thickened tendon sheath of the abductor pollicis longus and extensor pollicis brevis tendons within the first compartment

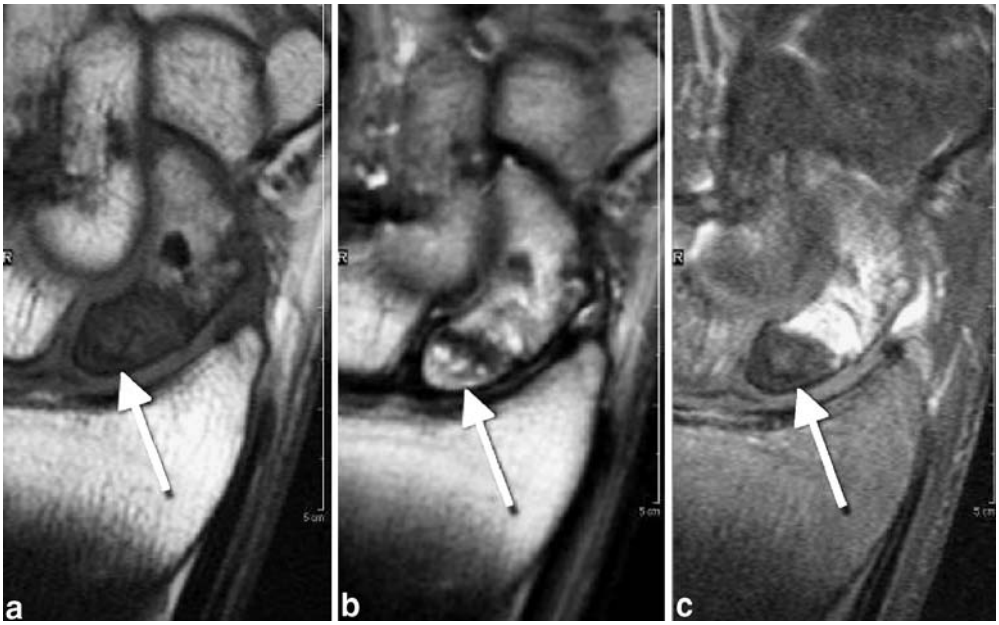

Fig. 7 Scaphoid pseudarthrosis with avascular necrosis of the proximal fragment. The proximal fragment (*arrow*) is hypointens on a coronal T1-weighted spin-echo image (**a**), mixed hyperintense on a coronal T2-weighted fast spin-echo image (**b**), and hypointense on a fat-suppressed gadolinium-enhanced T1-weighted spin-echo MR image (**c**)

the extensor retinaculum. The first compartment reaches at its distal end the radial styloid process and contains the abductor pollicis longus and extensor pollicis brevis tendon. The etiology of de Quervain's tenosynovitis is unknown; however, it may be caused by subclinical rheumatoid arthritis, myxedema, or anatomic variation consisting in a division of the compartment by an additional septum [36].

Bone marrow

MR imaging is extremely sensitive for bone marrow abnormalities. Bone marrow abnormalities in the lunate bone may be associated with avascular necrosis, any types of impaction syndrome or represent the beginning of an intraosseous ganglion.

Avascular necrosis of the proximal scaphoid pole

Avascularity of the proximal fragment is reported to be a critical determinant for the healing of acute scaphoid fractures and equally also for the outcome in treating established nonunions of the scaphoid [37]. Some authors [38, 39] have reported on the consistent correlation between low signal intensity on both T1-and T2-weighted MR images of the proximal fragment and poor vascularity. However, the value of unenhanced MR for assessment of pseudarthrosis is controversial. Cerezal et al. [40] have

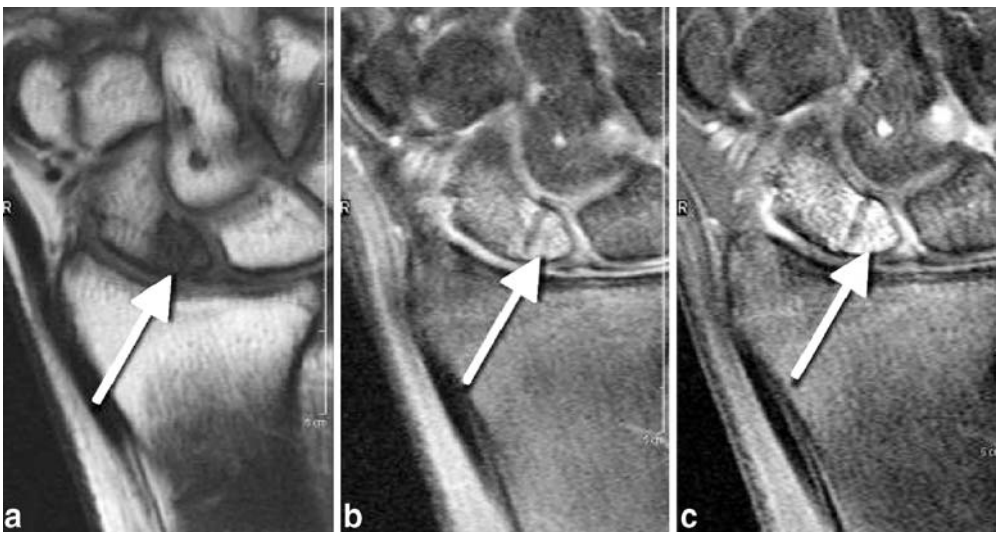

Fig. 8 Scaphoid pseudarthrosis with reparative changes in the proximal fragment. Hypointense proximal fragment on coronal T1-weighted image (**a**), hyperintense on proton-density-weighted fat-suppressed image (**b**), followed by enhancement on T1-weighted fat-suppressed MR image after gadolinium application (**c**) indicates that there is some vascularized tissue within the fragment

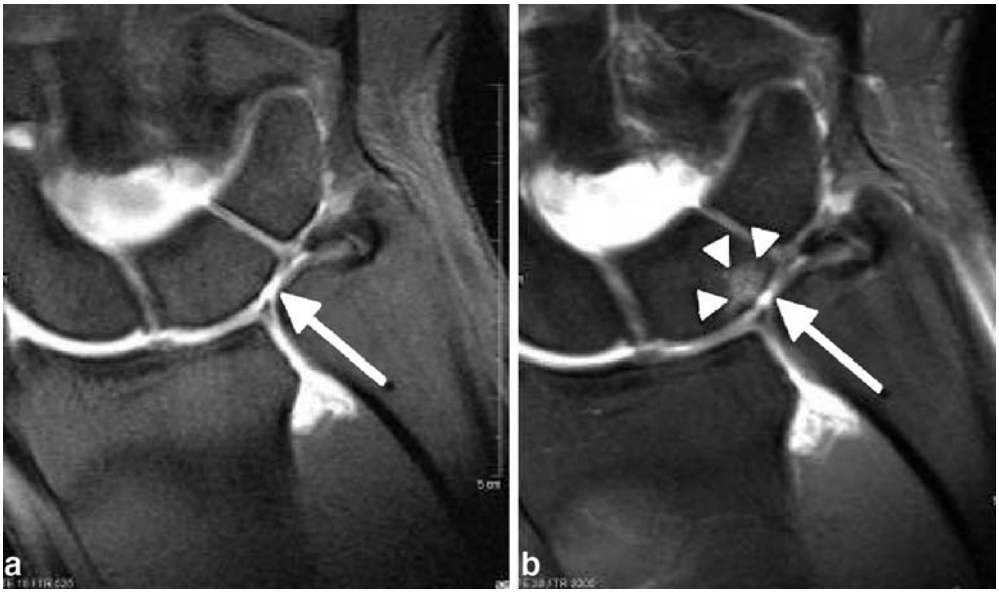

Fig. 9 Ulnar impaction syndrome. Coronal T1-weighted fat suppressed MR arthrogram (**a**) demonstrates a broad communicating triangular fibrocartilage tear, Palmer class 2 (*arrow*) and a cartilage defect opposite of the tear over the lunate. The coronal proton-density-weighted fat-suppressed MR arthrogram (**b**) demonstrates the characteristic focal signal intensity changes in the ulnar aspect of the lunate (*arrowheads*)

found that unenhanced MR assessments of vascularity were much less reliable, having only 36% sensitivity, 78% specificity and 86% accuracy. Gadolinium-enhanced MR imaging for assessment of proximal pole vascularity was found more reliable, with 66% sensitivity, 88% specificity and 83% accuracy. Thus, by now gadolinium-enhanced MR is considered the best technique for detecting established avascularity of bone in patients with pseudarthrosis (Fig. 7). Nevertheless, it is important to recognize that histopathological samples from an "avascular" proximal fragment also contain areas of vascularized bone in a patchy distribution. Therefore, enhancement of the proximal fragment of a scaphoid nonunion simply indicates the presence of some vascular tissue within the fragment (Fig. 8). This might well also correspond to some unspecific reactive inflammatory tissue originating from the nonunion site invading the proximal fragment rather than true spontaneous revascularisation or recovery from an avascular insult. Healing is still possible, but the evolution of an avascular necrosis cannot be ruled out. On the other hand, absence of enhancement does not indicate vascular necrosis of the proximal fragment when the bone marrow shows otherwise the normal fatty content of normal bones. There is a different enhancement pattern between early and chronic fracture patients. In acute fracture patients, enhancement of the distal pole is greater than that of the proximal. However, poor proximal vascularity of the proximal fragment is not an important

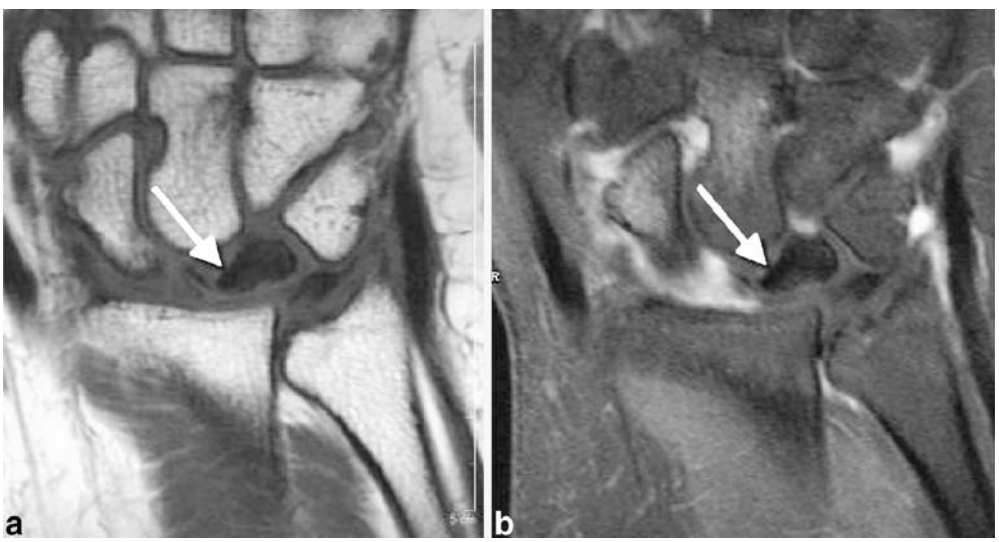

Fig. 10 Avascular necrosis of the lunate (Kienboeck's disease). The necrotic low signal intense lunate starts collapsing in the radial aspect (arrow). Coronal T1-weighted spin-echo image (**a**), corresponding T1-weighted fat-suppressed spin-echo image after gadolinium application (**b**) does not demonstrate any enhancement

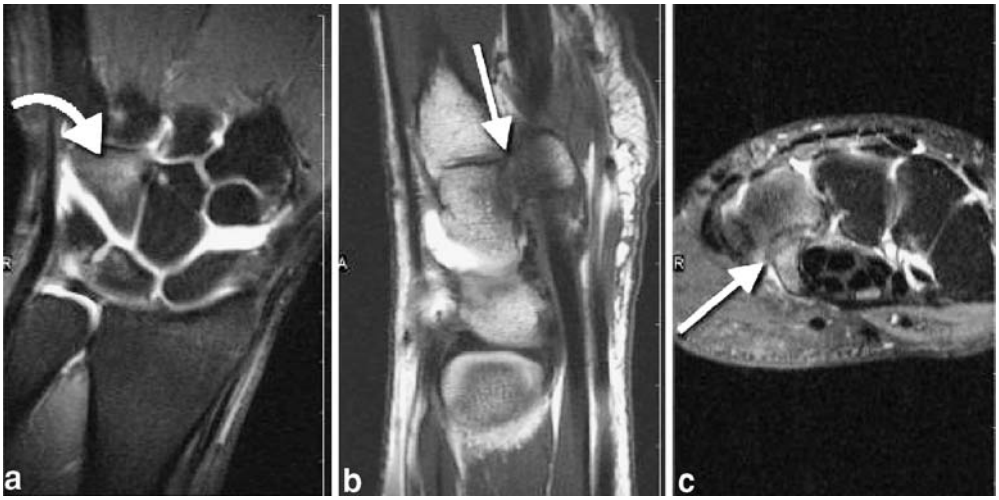

Fig. 11 Hamulus fracture. **a** Coronal proton-density-weighted fat-suppressed MR arthrogram. **b** Sagittal T1-weighted MR arthrogram. **c** Axial proton-density-weighted fat-suppressed MR arthrogram. Beneath bone bruise (*curved arrow*) with a reticular appearance a fracture with line distinct linear abnormalities (*arrow*) is shown at the base of the hamulus

determinant of union in fractures of the scaphoid [41]. In chronic fracture patients the enhancement pattern is reversed, as the proximal pole enhances to a greater degree than the distal pole [42].

Ulnar impaction

Ulnocarpal impaction syndrome has been recognized as a common clinical finding in patients with chronic ulnar-sided wrist pain and functional restriction of the ulnocarpal joint. Most cases of ulnar impaction syndrome have characteristic focal signal intensity changes in the ulnar aspect of the lunate (Fig. 9). The signal intensity often returns to normal after successful ulnar shortening [43].

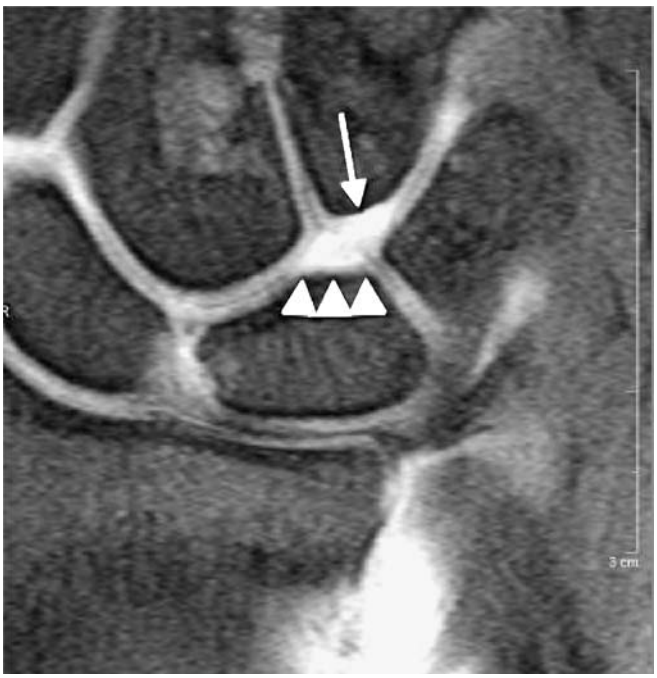

Fig. 12 Cartilage defect, hamate-lunate facet (type II lunate). Coronal proton-density-weighted fat-suppressed MR arthrogram demonstrates a cartilage defect (*arrow*) in the proximal pole of the hamate associated with a second facet (*arrowheads*) besides the one to the capitate

Kienböck's disease (avascular necrosis of the lunate)

In contrast to ulnar impaction abnormalities avascular necrosis of the lunate is characterized by signal changes starting in the proximal *radial* aspect of the lunate. The disease may progress and entail necrosis and collapse and/or fragmentation of the lunate [44] (Fig. 10), eventually leading to arthritic degeneration.

Occult fractures

Occult bone lesions (often referred to as bone bruises when posttraumatic) are seen at MR imaging as signal intensity abnormalities in the subchondral bone marrow and represent a heterogeneous group of injuries [45]. Bone bruises with a reticular appearance on MR images are often regarded as benign and self-limiting lesions, while fractures with distinct linear abnormalities (e.g., fracture of the hook of the hamate) (Fig. 11) are considered as more meaningful. MR imaging has been shown highly sensitive for detecting **fractures** of the scaphoid and other carpals not evident on plain radiographs [46]. However, to our knowledge it is not clear whether occult posttraumatic bone lesions, seen on MR images only, necessarily require the same treatment as fractures evident on plain films or CT images. If not, one may doubt on the clinical relevance of MR diagnoses of occult fractures and argue on its widespread compared with CT.

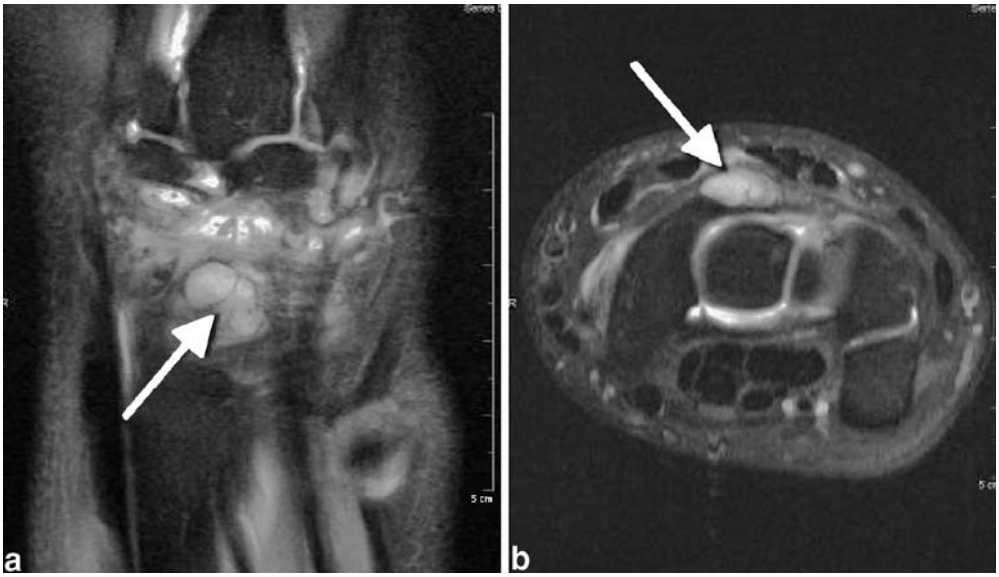

Fig. 13 Ganglion. A characteristic dorsal ganglion (*arrow*) in close vicinity to the scapholunate ligaments is shown on coronal (**a**) and axial proton-density-weighted fat-suppressed MR images (**b**)

Hyaline cartilage

Imaging of articular cartilage of the wrist is challenging and correct assessment of the cartilage surface has become mandatory for comprehensive decision making in reconstructive wrist surgery. In choosing from the various modalities of surgical wrist salvage procedures it is of utmost importance to locate the irreparable damage of the cartilage warranting fusion of this affected joint segment as well as reliably define the site of healthy and preserved joint components worth to be retained functional and mobile. This is decisive when to determine the extent of fusion following fractures of the distal radius. Moreover, it is important to choose between the variants of limited radiocarpal wrist fusion and total wrist arthrodesis [47]. Equally frequent and important is the decision between proximal row carpectomy and midcarpal (four-corner) arthrodesis when treating patients with Kienböck's disease and scapho lunate advanced collapse (SLAC) wrist [48–50]. In SLAC stage 2, by definition [51], and Kienböck's stage 3 [31] the cartilaginous surfaces of the capitate head and the lunate fossa of the radius are intact, allowing their direct painless articulation after simple resection of the scaphoid, lunate and triquetrum, the so-called proximal row carpectomy. This may not be equally appropriate in stage 3, with deterioration of cartilage on the head of the capitate along with the midcarpal joint. This condition may spare only the radio-lunate joint and necessitate scaphoid

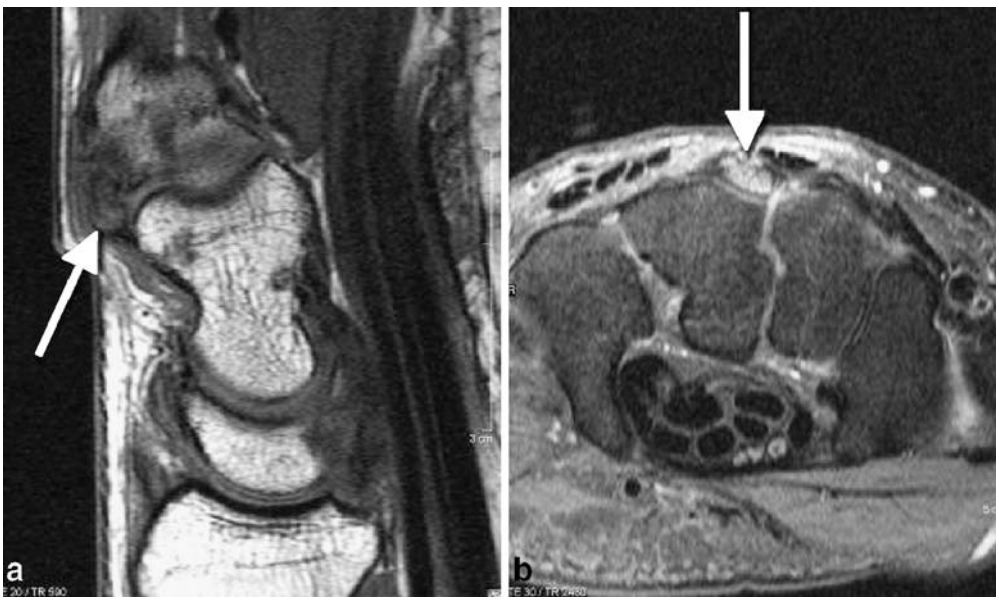

Fig. 14 Carpal boss (carpe bossu). **a** Sagittal T1-weighted spin-echo image along the radius, lunate, capitate and metatarsal III. **b** Axial proton-density-weighted fat-suppressed-spin-echo image. A super numerous bone (os styloideum) (*arrow*) with bone marrow changes is shown at the base of the metacarpal bone III

excision and surgical fusion of the destroyed midcarpal joint between lunate, triquetrum, capitate and hamate, the so-called four-corner-fusion [48, 50, 52].

There are only sparse data with regard to diagnostic performance of MRI for assessment of wrist cartilage [53–55]. Cartilage lesions of the radiocarpal and intercarpal joints are only to a limited degree routinely diagnosed with MR imaging or MR arthrography of the wrist, despite their clinical importance [54, 55]. This might be due to the fact that the hyaline articular cartilage layers of the radiocarpal and intercarpal joints are relatively thin [56], resulting in difficulties for their visualization. Additionally, the clinical usefulness of MR imaging is currently restricted by the long time it takes to obtain the high-spatial-resolution images necessary for adequate cartilage depiction [57]. Optimization of cartilage imaging with magnetic resonance imaging has evolved in two directions: quantitative techniques, such as T1-rho and T2-mapping [58], and morphologic techniques based on new imaging sequences and higher field strengths directly visualize cartilage structure and defects [14, 57].

Standard MR imaging at 1.5 T is relatively inaccurate for detecting and allowing description of focal articular cartilage defects in the radiocarpal joint [54]. Sensitivities in detection of focal cartilage lesions in the proximal carpal row range from 18% to 41%, and specificities ranging from 75% to 93% [54]. To increase the accuracy for cartilage lesions, the predilection sites for cartilage defects should be considered. The presence of a hamate-lunate facet, also called type II lunate with a second facet besides the one to the capitate, is associated with cartilage damage in the proximal pole of the hamate (Fig. 12) [55]. Special attention should be also paid at the pisotriquetral joint. The pisotriquetral joint is the third most common site of osteoarthritis in the wrist after the scaphotrapezial joint and the carpometacarpal joint [59, 60].

Miscellaneous

Ganglion

A ganglion (Fig. 13) is a lesion of unknown origin that arises in the paraarticular tissues. Ganglia about the wrist are common; they may be asymptomatic or may cause tenderness or pain due to pressure and inflammation of adjacent structures, such as tendons and tendon sheaths, sometimes irritation of compressed and distorted sensory nerve branches in larger lesions. Not all wrist ganglia are readily visible or palpable and in absence of clinical confirmative findings but suggestive patient history the term “occult wrist ganglion” has been created [61]. In the pre-sonographic and pre-MR era this diagnosis was related to small intracapsular wrist ganglia confirmed only at the time of surgery or only from biopsy of the excised capsule overlying the scapholunate interval. Nowadays, MR imaging and ultrasound are equally effective for detecting occult carpal ganglia [62]. Ganglia in the wrist have a characteristic location close to the scapholunate ligament [63].

Carpe bossu (carpal boss)

Carpe bossu (Fig. 14) is a bony protuberance of a carpometacarpal joint II and III [64]. It may caused by a super numerous bone (os styloideum) or more often by an osteophyte at the base of the metacarpal bone II or III originating from the ca0rpometacarpal joint, which may be dorsally narrow and degenerated. Sometimes this condition is accompanied by a small ganglion cyst. The latter or associated bone marrow changes are visible.

Nerve entrapment

Carpal tunnel syndrome is the most common among the entrapment neuropathies. It is thought to arise secondary to a wide variety of conditions, eventually leading to chronic tenosynovitis, including repetitive strain but also following space-occupying lesions [44]. The diagnosis is usually made clinically. Imaging is therefore rarely required unless a space occupying lesion such as a ganglion is suspected.

References

1. Berna-Serna JD, Martinez F, Reus M, Alonso J, Domenech-Ratto G (2006) Wrist arthrography: a simple method. Eur Radiol 16:469–472
2. Schmitt R, Froehner S, Coblenz G, Christopoulos G (2006) Carpal instability. Eur Radiol DOI 10.1007/s00330-006-0161-1
3. Golimbu CN, Firooznia H, Melone CP Jr, Rafii M, Weinreb J, Leber C (1989) Tears of the triangular fibrocartilage of the wrist: MR imaging. Radiology 173:731–733
4. Saupe N, Prussmann KP, Luechinger R, Bosiger P, Marincek B, Weishaupt D (2005) MR imaging of the wrist: comparison between 1.5- and 3-T MR imaging—preliminary experience. Radiology 234:256–264

5. Scheck RJ, Romagnolo A, Hierner R, Pfluger T, Wilhelm K, Hahn K (1999) The carpal ligaments in MR arthrography of the wrist: correlation with standard MRI and wrist arthroscopy. J Magn Reson Imaging 9:468–474
6. Zanetti M, Bram J, Hodler J (1997) Triangular fibrocartilage and intercarpal ligaments of the wrist: does MR arthrography improve standard MRI? J Magn Reson Imaging 7:590–594
7. Linscheid RL, Dobyns JH, Beabout JW, Bryan RS (2002) Traumatic instability of the wrist: diagnosis, classification, and pathomechanics. J Bone Joint Surg Am 84-A:142
8. Zanetti M, Hodler J, Gilula LA (1998) Assessment of dorsal or ventral intercalated segmental instability configurations of the wrist: reliability of sagittal MR images. Radiology 206:339–345
9. Haims AH, Schweitzer ME, Morrison WB et al (2003) Internal derangement of the wrist: indirect MR arthrography versus unenhanced MR imaging. Radiology 227:701–707
10. Steinbach LS, Palmer WE, Schweitzer ME (2002) Special focus session. MR arthrography. Radiographics 22: 1223–1246
11. Bergin D, Schweitzer ME (2003) Indirect magnetic resonance arthrography. Skeletal Radiol 32:551–558
12. Gold GE, Fuller SE, Hargreaves BA, Stevens KJ, Beaulieu CF (2005) Driven equilibrium magnetic resonance imaging of articular cartilage: initial clinical experience. J Magn Reson Imaging 21:476–481
13. Gold GE, Han E, Stainsby J, Wright G, Brittain J, Beaulieu C (2004) Musculoskeletal MRI at 3.0 T: relaxation times and image contrast. AJR Am J Roentgenol 183:343–351
14. Gold GE, Suh B, Sawyer-Glover A, Beaulieu C (2004) Musculoskeletal MRI at 3.0 T: initial clinical experience. AJR Am J Roentgenol 183:1479–1486
15. Link TM, Sell CA, Masi JN et al (2006) 3.0 vs 1.5 T MRI in the detection of focal cartilage pathology-ROC analysis in an experimental model. Osteoarthritis Cartilage 14:63–70
16. Zlatkin MB, Chao PC, Osterman AL, Schnall MD, Dalinka MK, Kressel HY (1989) Chronic wrist pain: evaluation with high-resolution MR imaging. Radiology 173:723–729
17. Johnstone DJ, Thorogood S, Smith WH, Scott TD (1997) A comparison of magnetic resonance imaging and arthroscopy in the investigation of chronic wrist pain. J Hand Surg [Br] 22:714–718
18. Lester B, Halbrecht J, Levy IM, Gaudinez R (1995) "Press test" for office diagnosis of triangular fibrocartilage complex tears of the wrist. Ann Plast Surg 35:41–45
19. Shionova K, Nakamura R, Imaeda T, Makino N (1998) Arthrography is superior to magnetic resonance imaging for diagnosing injuries of the triangular fibrocartilage. J Hand Surg 23B:402–405
20. Scheck RJ, Kubitzek C, Hierner R et al (1997) The scapholunate interosseous ligament in MR arthrography of the wrist: correlation with non-enhanced MRI and wrist arthroscopy. Skeletal Radiol 26:263–271
21. Schmitt R, Christopoulos G, Meier R et al (2003) [Direct MR arthrography of the wrist in comparison with arthroscopy: a prospective study on 125 patients]. Rofo 175:911–919
22. Braun H, Kenn W, Schneider S, Graf M, Sandstede J, Hahn D (2003) [Direct MR arthrography of the wrist- value in detecting complete and partial defects of intrinsic ligaments and the TFCC in comparison with arthroscopy]. Rofo 175:1515–1524
23. Haims AH, Schweitzer ME, Morrison WB et al (2002) Limitations of MR imaging in the diagnosis of peripheral tears of the triangular fibrocartilage of the wrist. AJR Am J Roentgenol 178:419–422
24. Palmer AK (1989) Triangular fibrocartilage complex lesions: a classification. J Hand Surg 14A:594–606
25. Zanetti M, Linkous MD, Gilula LA, Hodler J (2000) Characteristics of triangular fibrocartilage defects in symptomatic and contralateral asymptomatic wrists. Radiology 216:840–845
26. Oneson SR, Timins ME, Scales LM, Erickson SJ, Chamoy L (1997) MR imaging diagnosis of triangular fibrocartilage pathology with arthroscopic correlation. AJR 168:1513–1518
27. Trumble TE, Gilbert M, Vedder N (1997) Isolated tears of the triangular fibrocartilage: management by early arthroscopic repair. J Hand Surg 22A:57–65
28. Benjamin M, Evans EJ, Pemberton DJ (1990) Histological studies on the triangular fibrocartilage complex of the wrist. J Anat 172:59–67
29. Totterman SM, Miller RJ, McCance SE, Meyers SP (1996) Lesions of the triangular fibrocartilage complex: MR findings with a three-dimensional gradient-recalled-echo sequence. Radiology 199:227–232
30. Ruegger C, Schmid M, Pfirrmann CW, Nagy L, Gilula LA, Zanetti M (2007) Peripheral triangular fibrocartilage tears: depiction with distal radioulnar joint MR arthrography. AJR Am J Roentgenol (in press)
31. Lichtmann D, Alexander A (1996) The wrist and its disorders, 2 edn. WB Saunders, Philadelphia
32. Berger RA (2001) The anatomy of the ligaments of the wrist and distal radioulnar joints. Clin Orthop Relat Res 383:32–40
33. Viegas SF, Ballantyne G (1987) Attritional lesions of the wrist joint. J Hand Surg [Am] 12:1025–1029
34. Linkous MD, Pierce SD, Gilula LA (2000) Scapholunate ligamentous communicating defects in symptomatic and asymptomatic wrists: characteristics. Radiology 216:846–850
35. Allende C, Le Viet D (2005) Extensor carpi ulnaris problems at the wrist—classification, surgical treatment and results. J Hand Surg [Br] 30:265–272
36. Glajchen N, Schweitzer M (1996) MRI features in de Quervain's tenosynovitis of the wrist. Skeletal Radiol 25:63–65
37. Singh AK, Davis TR, Dawson JS, Oni JA, Downing ND (2004) Gadolinium enhanced MR assessment of proximal fragment vascularity in nonunions after scaphoid fracture: does it predict the outcome of reconstructive surgery? J Hand Surg [Br] 29:444–448
38. Perlik PC, Guilford WB (1991) Magnetic resonance imaging to assess vascularity of scaphoid nonunions. J Hand Surg [Am] 16:479–484
39. Trumble TE (1990) Avascular necrosis after scaphoid fracture: a correlation of magnetic resonance imaging and histology. J Hand Surg [Am] 15:557–564
40. Cerezal L, Abascal F, Canga A, Garcia-Valtuille R, Bustamante M, del Pinal F (2000) Usefulness of gadolinium-enhanced MR imaging in the evaluation of the vascularity of scaphoid nonunions. AJR Am J Roentgenol 174:141–149

41. Dawson JS, Martel AL, Davis TR (2001) Scaphoid blood flow and acute fracture healing. A dynamic MRI study with enhancement with gadolinium. J Bone Joint Surg Br 83:809–814
42. Munk PL, Lee MJ, Janzen DL et al (1998) Gadolinium-enhanced dynamic MRI of the fractured carpal scaphoid: preliminary results. Australas Radiol 42:10–15
43. Imaeda T, Nakamura R, Shionoya K, Makino N (1996) Ulnar impaction syndrome: MR imaging findings. Radiology 201:495–500
44. Schmitt R, Christopoulos G, Kalb K et al (2005) [Differential diagnosis of the signal-compromised lunate in MRI]. Rofo 177:358–366
45. Boks SS, Vroegindeweij D, Koes BW, Hunink MG, Bierma-Zeinstra SM (2006) Follow-up of occult bone lesions detected at mr imaging: systematic review. Radiology 238: 853–862
46. Breitenseher MJ, Metz VM, Gilula LA et al (1997) Radiographically occult scaphoid fractures: value of MR imaging in detection. Radiology 203:245–250
47. Nagy L (2005) Salvage of post-traumatic arthritis following distal radius fracture. Hand Clin 21:489–498
48. Cohen MS, Kozin SH (2001) Degenerative arthritis of the wrist: proximal row carpectomy versus scaphoid excision and four-corner arthrodesis. J Hand Surg [Am] 26:94–104
49. Tomaino MM, Miller RJ, Cole I, Burton RI (1994) Scapholunate advanced collapse wrist: proximal row carpectomy or limited wrist arthrodesis with scaphoid excision? J Hand Surg [Am] 19:134–142
50. Wyrick JD, Stern PJ, Kiefhaber TR (1995) Motion-preserving procedures in the treatment of scapholunate advanced collapse wrist: proximal row carpectomy versus four-corner arthrodesis. J Hand Surg [Am] 20:965–970
51. Watson HK, Ballet FL (1984) The SLAC wrist: scapholunate advanced collapse pattern of degenerative arthritis. J Hand Surg [Am] 9:358–365
52. Watson HK, Goodman ML, Johnson TR (1981) Limited wrist arthrodesis. Part II: Intercarpal and radiocarpal combinations. J Hand Surg [Am] 6:223–233
53. Bordalo-Rodrigues M, Schweitzer M, Bergin D, Culp R, Barakat MS (2005) Lunate chondromalacia: evaluation of routine MRI sequences. AJR Am J Roentgenol 184:1464–1469
54. Haims AH, Moore AE, Schweitzer ME et al (2004) MRI in the diagnosis of cartilage injury in the wrist. AJR Am J Roentgenol 182:1267–1270
55. Pfirrmann CW, Theumann NH, Chung CB, Trudell DJ, Resnick D (2002) The hamatolunate facet: characterization and association with cartilage lesions-magnetic resonance arthrography and anatomic correlation in cadaveric wrists. Skeletal Radiol 31:451–456
56. Peterfy CG, van Dijke CF, Lu Y et al (1995) Quantification of the volume of articular cartilage in the metacarpophalangeal joints of the hand: accuracy and precision of three-dimensional MR imaging. AJR Am J Roentgenol 165:371–375
57. Hargreaves BA, Gold GE, Beaulieu CF, Vasanawala SS, Nishimura DG, Pauly JM (2003) Comparison of new sequences for high-resolution cartilage imaging. Magn Reson Med 49: 700–709
58. Dunn TC, Lu Y, Jin H, Ries MD, Majumdar S (2004) T2 relaxation time of cartilage at MR imaging: comparison with severity of knee osteoarthritis. Radiology 232:592–598
59. Fischer E (1988) [Piso-triquetral arthrosis and the so-called pisiform secundarium]. Radiologe 28:338–344
60. Theumann NH, Pfirrmann CW, Chung CB, Antonio GE, Trudell DJ, Resnick D (2002) Pisotriquetral joint: assessment with MR imaging and MR arthrography. Radiology 222:763–770
61. Gunther SF (1985) Dorsal wrist pain and the occult scapholunate ganglion. J Hand Surg [Am] 10:697–703
62. Cardinal E, Buckwalter KA, Capello WN, Duval N (1996) US of the snapping iliopsoas tendon. Radiology 198:521–522
63. el-Noueam KI, Schweitzer ME, Blasbalg R et al (1999) Is a subset of wrist ganglia the sequela of internal derangements of the wrist joint? MR imaging findings. Radiology 212: 537–540
64. Conway WF, Destouet JM, Gilula LA, Bellinghausen HW, Weeks PM (1985) The carpal boss: an overview of radiographic evaluation. Radiology 156: 29–31
65. Hobby JL, Tom BD, Bearcroft PW, Dixon AK (2001) Magnetic resonance imaging of the wrist: diagnostic performance statistics. Clin Radiol 56: 50–57
66. Pederzini L, Luchetti R, Soragni O et al (1992) Evaluation of the triangular fibrocartilage complex tears by arthroscopy, arthrography, and magnetic resonance imaging. Arthroscopy 8:191–197
67. Schweitzer ME, Brahme SK, Hodler J et al (1992) Chronic wrist pain: spin-echo and short tau inversion recovery MR imaging and conventional and MR arthrography. Radiology 182:205–211
68. Potter HG, Asnis-Ernberg L, Weiland AJ, Hotchkiss RN, Peterson MG, McCormack RR Jr (1997) The utility of high-resolution magnetic resonance imaging in the evaluation of the triangular fibrocartilage complex of the wrist. J Bone Joint Surg 79A: 1675–1684
69. Totterman SM, Miller R, Wasserman B, Blebea JS, Rubens DJ (1993) Intrinsic and extrinsic carpal ligaments: evaluation by three-dimensional Fourier transform MR imaging. AJR Am J Roentgenol 160:117–123